A Novel AFM Chip for Fountain Pen Nanolithography - Design and Microfabrication

Keun-Ho Kim, Nicolaie Moldovan, Changhong Ke and Horacio D. Espinosa*
Department of Mechanical Engineering, Northwestern University, 2145 Sheridan Road, Evanston, IL 60208, U.S.A.

ABSTRACT

A novel atomic force microscopy (AFM) probe has been developed to expand the capability and applications of dip-pen nanolithography (DPN) technology. This new probe has integrated microchannels and reservoirs for continuous ink feed, which allow "fountain-pen" writing called "Fountain Pen Nanolithography" (FPN). Ink is transported from the reservoirs through the microchannels and eventually dispensed onto substrates via a volcano-like dispensing tip. Numerical simulations have been performed to select optimal materials and suitable tip shapes providing a stable fluid-air interface in the tip. Microchannel and dispensing tip have been fabricated by surface micromachining, in particular employing 3 layers of thin films. Fluid flow through the microchannels has been experimentally examined. The probe was used to write on a gold substrate.

*Corresponding author: espinosa@northwestern.edu

INTRODUCTION

Nanoscale patterning capabilities are important to construct functional nanostructures on surfaces via bottom-up approach. Among nanopatterning methodologies, dip-pen nanolithography (DPN) is a direct-write method to produce nanostructures with high resolution of less than 20 nm [1]. In this method, an atomic force microscope (AFM) tip is coated with molecules or "inks" and brought into contact with a surface or "paper" to deposit the coated molecules. A water meniscus formed between an AFM tip and a surface is proposed as the transfer mechanism that enables the delivery of molecules from the tip to the surface. DPN was originally demonstrated for patterning monolayers of alkanethiol on gold surfaces, and subsequently expanded to patterning biomolecules [2,3] and inorganic materials [4-8]. In DPN, molecules are coated either by dipping an AFM tip into a solution containing the molecules or by evaporation from a source. When patterning of large areas or complex structures is required, the tips need to be replenished periodically, leading to additional time-consuming steps and strongly limiting the versatility of the technique. In an effort to overcome this drawback, several studies have been reported on continuous ink feeding. A pulled micropipette with a small aperture was used to continuously deliver liquid substance to a substrate enabling a nanoscale control of the chemical reaction [9-11]. However, pulled micropipettes typically suffer from irregular aperture size and low reproducibility. Another approach was to microfabricate an aperture at the apex of a hollow pyramidal tip, utilizing the back side of the tip as a reservoir [12]. However, the resolution is not competitive with DPN since the feature size is dependent on the aperture size. Here we report a novel AFM probe, so-called nano-fountain probe, integrated with microchannels and an ink-dispensing tip, achieving both continuous ink feeding and high resolution writing.

DEVICE DESIGN

A rectangular-shaped cantilever with a round free end is combined with a microchannel and a dispensing tip. The dimensions of the cantilever are 1.5 µm, 20 µm, and 300-500 µm for thickness, width and length, respectively. Along the edge of the cantilever, a 5-µm-wide and half-a-micron-deep microchannel is embedded. A 4-µm-high volcano-like dispensing tip is integrated at the free end, which has an annular aperture around a core AFM tip. The aperture is connected to the microchannels for ink delivery. Five cantilevers with different lengths have been microfabricated on a silicon chip, on which an on-chip reservoir has been integrated to store ink. The schematic of the device is shown in Figure 1. The chip has been designed to be mounted onto commercial AFMs to utilize their scanner and deflection detection scheme. Once a solution containing a chemical of interest is placed in the reservoir, it is delivered by capillary action to the dispensing tip, stopping near the end of the core tip to form an air-liquid interface (Figure 2a). As the tip is brought into contact with a surface, molecules delivered to the interface diffuse along the core tip to the substrate depositing patterns as in DPN [1].

In order to assess the feasibility of capillary action for ink delivery, numerical simulations have been performed. The channel considered was 0.5 µm high and 500 µm long. A series of simulations were carried out using commercial software (CFD-ACE+, CFDRC) for materials with different wetting angles (Figure 2). Our calculations have shown that ink can flow through the channel by the capillary force resulting from the small channel dimensions. The results have also shown how the equilibrium liquid-air interface is determined by both the geometry of the device and the contact angles of the liquid on the solid wall surfaces. For a certain combination of materials for the core tip and the surrounding shell, a stable liquid-air interface is attainable (Figure 2a). By contrast, a highly hydrophilic tip and shell results in overflow out of the microchannel (Figure 2b), which is not desirable in DPN writing.

FABRICATION

Surface micromachining has been used to microfabricate an AFM cantilever integrated with a microchannel and a dispensing tip. Three layers of thin films are stacked by low-pressure chemical vapor deposition (LPCVD) processes. First, a low-stress silicon nitride layer (~3000 Å) has been deposited on a {100} silicon wafer. Subsequently, a low temperature oxide (LTO) layer (~5000 Å), which will later serve as a sacrificial layer, is deposited through LPCVD. Finally, deposition of composite layer of stoichiometric (~500 Å) and low-stress (~1500 Å) LPCVD nitride for stress compensation completes a trilayer structure. This SiN/SiO/SiN trilayer will serve as foundation for building both channels and tips in the following steps.

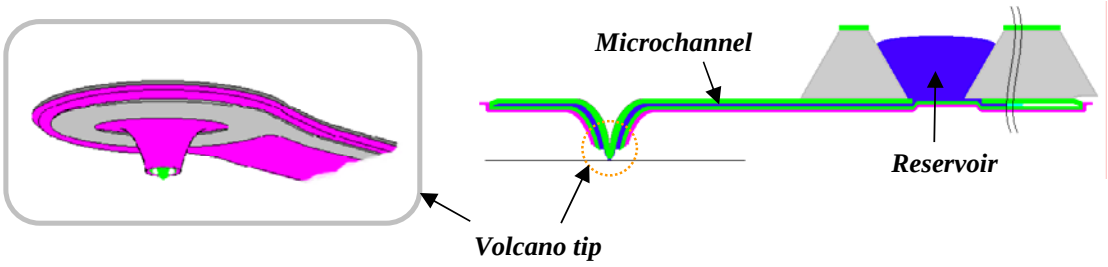

Figure 1. Novel nano-fountain probe with a volcano tip and a reservoir.

The shape of a cantilever has been defined by photolithographic steps, followed by reactive ion etch (RIE) to expose a supporting substrate of Si on the front side of the wafer. From the side walls defined by the RIE, the middle oxide of the trilayer is etched in buffered HF until the undercut reaches ~5 µm (Figure 3a). This undercut forms a lateral trench along the edge of the not-yet-released cantilever and determines the width of the microchannels. In addition, the height of the microchannels is determined by the thickness of the LTO layer. In the following thermal oxidation process, only exposed silicon areas are oxidized leading to bird's beak shape at the boundaries of the cantilever, which closes the lateral trench by lifting the edge of the bottom nitride layer (Figure 3b). Subsequently, deposition of a low-stress nitride layer (2000 Å) to ensure sealing completes an embedded microchannel (Figure 3c). Figure 4 shows an integrated microchannel in a released cantilever.

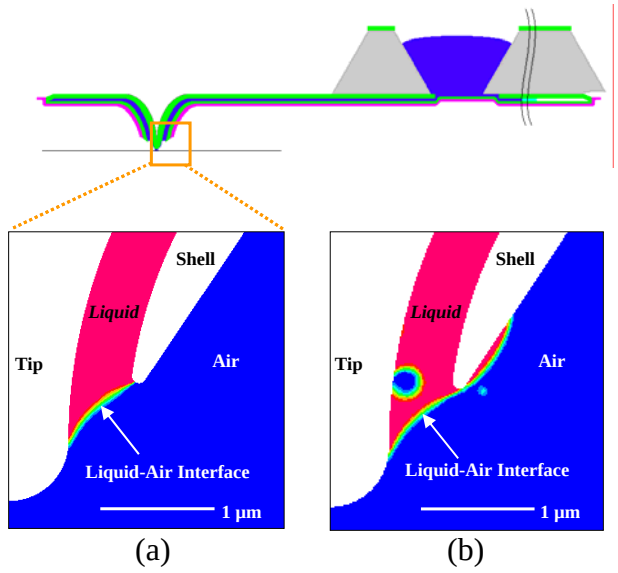

Figure 2. Liquid-air interface at the tip for two different combinations of tip and microchannel materials. The contact angles of the fluid with the tip and shell are: (a) 20° and 65°, respectively (SiO_2 tip and Si_3N_4 shell, (b) 20° for both (SiO_2 tip and shell)

In order to implement a volcano-like dispensing tip, a crystalline Si tip, which will later serve as a mold, is created prior to the deposition of the SiN/SiO/SiN trilayer. An LPCVD silicon nitride layer is deposited onto the silicon wafer, and subsequently patterned to define a precursor cap through photolithographic and RIE steps. The tip is formed by wet etching in a solution of $HF/CH_3COOH/HNO_3$ or potassium hydroxide (KOH), which undercuts the cap to form a tip (Figure 5a). After removing the cap, one micron of oxide is thermally grown at low temperature (950 °C) to improve tip sharpness (Figure 5b). We applied well-known recipes that take advantage of stress-induced oxidation reduction [13,14]. The oxide was subsequently removed in buffered HF, leaving a sharpened tip. The aforementioned trilayer and the sealing layer are conformally deposited over the tip while fabrication steps for a microchannel are carried out (Figure 5c). Once the microchannel is formed, photoresist is spin-coated on top of the structure, and RIE is performed in such a way that photoresist only on the end of the tip is etched away. After this step, a portion of the top nitride at the end of the tip is exposed to plasma and etched until the middle oxide beneath is exposed. Subsequently, the wafer is immersed into buffered HF

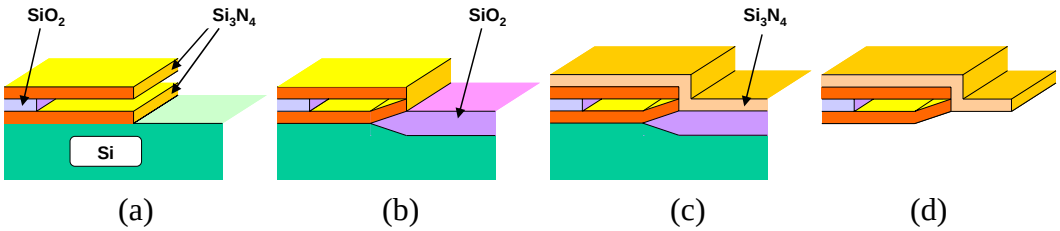

Figure 3. Microfabrication steps for microchannels.

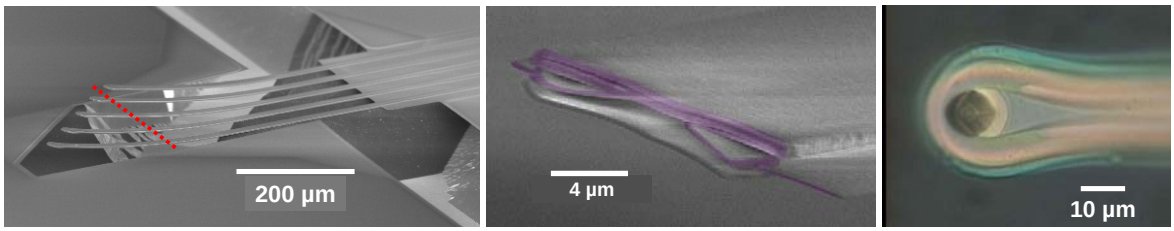

(a) (b) (c)

Figure 4. (a) SEM micrographs for parallel arrays of released cantilevers, (b) cross-section of a cantilever showing embedded microchannels, (c) optical micrograph of a cantilever with a microchannel along the edge and a tip in dark circle.

to etch the oxide layer, completing a volcano-like nitride tip and making connection to the microchannels (Figure 5d). Figure 6 shows completed dispensing tips. The cantilever integrated with the microchannel and dispensing tip is released by bulk etching of the Si substrate in a solution of KOH, through which an on-chip reservoir and handling part are formed simultaneously. The chips are microfabricated as arrays on a silicon wafer in such a way that they can be clipped off from the wafer and mounted into commercial AFMs.

EXPERIMENTS AND RESULTS

Proof-of-concept experiments have been performed to examine the suitability of capillary action for ink delivery through the microchannel. A solution of fluorescent dye in deionized water was placed in the on-chip reservoir, in which no pressure was applied. It was observed that the microchannels were filled with the solution under a fluorescence microscope (Figure 7). This experiment demonstrates that liquid transport from the reservoir through the microchannels is achievable by capillary force alone. The same processes were repeated with commonly-used inks

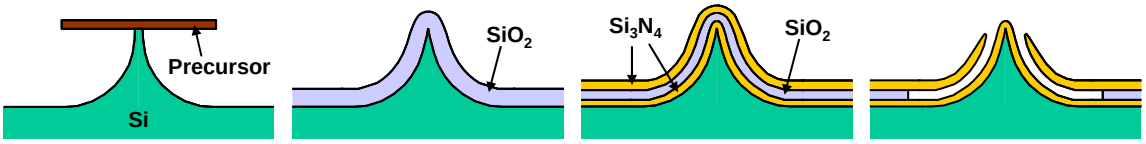

(a) (b) (c) (d)

Figure 5. Microfabrication steps for volcano-like dispensing tip.

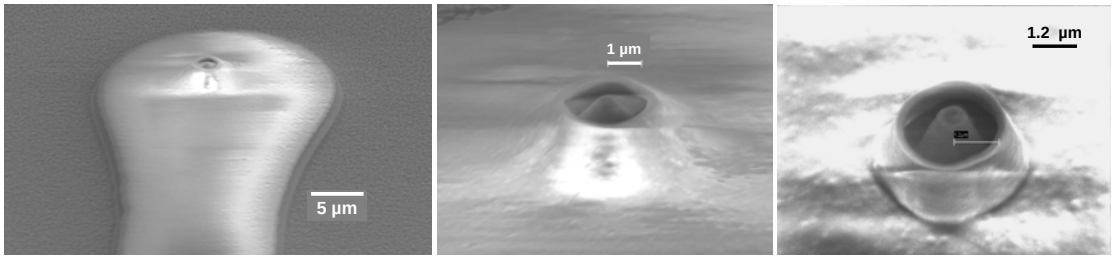

(a) (b) (c)

Figure 6. (a) SEM micrograph of a cantilever with an embedded microchannel and a volcano tip (prior to release). Dispensing tips: mold tips were etched by a solution of (b) $HF/CH_3COOH/HNO_3$ and (c) KOH.

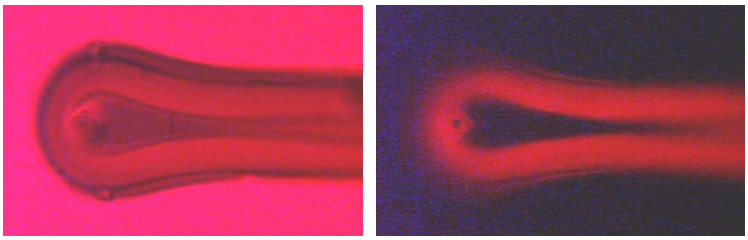

(a) (b)

Figure 7. Microchannels filled with a solution of fluorescence dye: (a) optical micrograph, (b) fluorescence optical micrograph; lighter color on filled fluorescing microchannels.

in DPN: saturated solutions of 1-octadecanethiol (ODT) or 16-mercaptohexadecanoic acid (MHA) in acetonitrile, ethanol, or methanol. For these DPN inks, regular optical microscopy was used to inspect the microchannel. Results with all of the solutions showed that the microchannel was completely filled by capillarity.

To evaluate the imaging capability of the developed probe, it was mounted to a commercial AFM (Dimension 3100, Digital Instruments). Scanning was performed over a standard calibration substrate which has arrays of 10 x 10 μm^2 squares with a height of 80 nm. Topography and lateral force images were obtained in contact mode operation (Figure 8a) and they showed good agreement with images obtained with commercial AFM probes. This experiment substantiates that the developed device can be used for imaging without changing to regular probes after writing.

Fountain-pen mode writing is currently possible provided that the end part of the core tip is primed with a solution. For priming, an ink such as saturated solution of MHA in acetonitrile was supplied to the reservoir, which, by observation under an optical microscope, fed the microchannels by capillarity. A Au-coated (50 nm) Si substrate was prepared by e-beam evaporation. The probe was mounted into the AFM and brought into contact with a spread droplet of the same solution that was placed near a target write area on the substrate. Then, the tip was moved onto a clean area and swept over the substrate to deposit patterns at a 0.03 µm/s scan rate at 50% relative humidity. Figure 8b shows deposited patterns. We think that the liquid-air interface at the end of the dispensing tip is formed a little far from the contact point of the tip with the substrate, so that a water meniscus cannot reach up to the interface, leading to failure in delivery from the interface to the substrate. Priming provides continuous coating ranging from

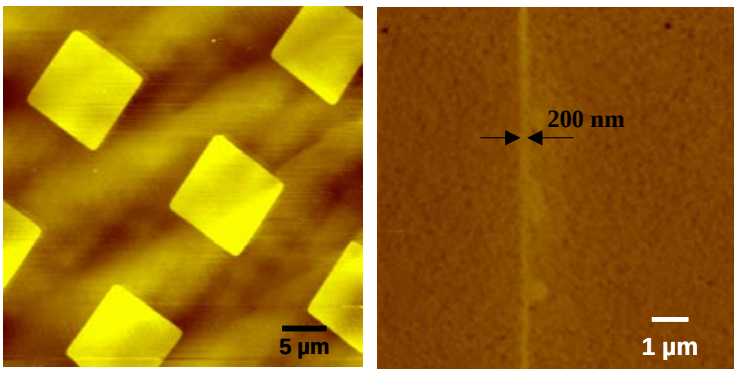

(a) (b)

Figure 8. (a) Topographic AFM image by the nano-fountain probe. (b) Lateral force image of a line and dots generated and scanned by the probe.

the interface to the contact point. The minimum feature size achieved so far is ~200 nm, which is larger by one order of magnitude than that of conventional DPN because of the configuration of the dispensing tip. As the silicon nitride conformally covers the sharp tip, the radius increases proportional to the film thickness. Revised tips with better sharpness as well as non-priming tips are under development.

CONCLUSIONS

A unique AFM probe integrated with reservoir, microchannels and a dispensing tip has been designed and fabricated using surface micromachining technology. Numerical simulations have been performed for selection of proper materials and geometries. A commercial AFM-mountable chip with such probes, which are capable of continuous ink feeding and high-resolution writing, has been microfabricated and preliminary tests have been performed.

ACKNOWLEDGEMENTS

This project is supported by the National Science Foundation - Nanoscale Science and Engineering Center (NSEC) at Northwestern University under Award Number EEC-0118025. Special thanks are due to Chad Mirkin and his group for many insightful discussions about DPN technology. The authors would like to acknowledge Microfabrication Applications Laboratory (MAL) of the University of Illinois at Chicago and Materials Processing and Crystal Growth Facility (MPCGF) of Northwestern University and Northwestern University Atomic- and Nanoscale Characterization Experimental (NU*ANCE*) Center.

REFERENCES

1. R. D. Piner, J. Zhu, F. Xu, S. Hong and C. A. Mirkin, *Science* **283**, 661 (1999).
2. K.-B. Lee, S.-J. Park, C. A. Mirkin, J. C. Smith and M. Mrksich, *Science* **295**, 1702 (2002).
3. L. M. Demers, D. S. Ginger, S.-J. Park, Z. Li, S.-W. Chung and C. A. Mirkin, *Science* **296**, 1836 (2002).
4. A. Ivanisevic and C. A. Mirkin, *J. Am. Chem. Soc.* **123**, 7887 (2001).
5. M. Su, X. Liu, S.-Y. Li, V. P. Dravid and C. A. Mirkin, *J. Am. Chem. Soc.* **124**, 1560 (2002).
6. B. W. Maynor, Y. Li and J. Liu, *Langmuir* **17**, 2575 (2001).
7. Y. Li, B. W. Maynor and J. Liu, *Langmuir* **123**, 2105 (2001).
8. L. Fu, X. Liu, Y. Zhang, V. P. Dravid, C. A. Mirkin, *Nano Lett.* **3**, 757 (2003).
9. A. Lewis, Y. Kheifetz, E. Shambrodt, A. Radko and E. Khatchatryan, *Appl. Phys. Lett.* **75**, 2689 (1999).
10. H. Taha, R. S. Marks, L. A. Gheber, I. Rousso, J. Newman, C. Sukenik, A. Lewis, *Appl. Phys. Lett.* **83**, 1041 (2003).
11. M.-H. Hong, K. H. Kim, J. Bae and W. Jhe, *Appl. Phys. Lett.* **77**, 2604 (2000).
12. A. Meister, S. Jeney, M. Liley, T. Akiyama, U. Staufer, N. F. de Rooij and H. Heinzelmann, *Proc. MNE 2002, Lugano, Switzerland*.
13. R. B. Marcus, T. S. Ravi, T. Gmitter, K. Chin, D. Liu, W. J. Orvis, R. D. Ciarlo, C. E. Hunt and J. Trujillo, *Appl. Phys. Lett.* **56**, 236 (1990).
14. T. S. Ravi, R. B. Marcus and D. Liu, *J. Vac. Sci. Technol.* **B9**, 2733 (1991).